Special Article

Stable Xenon CT Cerebral Blood Flow Imaging: Rationale for and Role in Clinical Decision Making

David W. Johnson,[1] Warren A. Stringer,[2] Michael P. Marks,[3] Howard Yonas,[4] Walter F. Good,[5] and David Gur[5]

The stable xenon CT method of measuring cerebral blood flow has been investigated in research studies for over 10 years. Recently, it has been gaining clinical acceptance, primarily owing to a combination of several unique advantages it holds over other cerebral blood flow measurement techniques. The accuracy of this technique in quantifying low cerebral blood flow gives it a unique application in cases of brain death and acute stroke and it can be repeated after an interval of 20 min, making it possible to evaluate autoregulation and cerebrovascular reserve. Furthermore, cerebral blood flow information is directly coupled to CT anatomy. Although it is more difficult to administer than a standard CT scan, careful monitoring can ensure patient safety during the examination. In this article we review the physiologic and technical bases for the clinical application of xenon CT–derived quantitative cerebral blood flow information and discuss the advantages and disadvantages of the technique. We also describe its current clinical applications, including its usefulness in the evaluation of acute stroke, occlusive vascular disease, carotid occlusion testing, vasospasm, arteriovenous malformations, and head trauma management.

History

The radiodensity of xenon (atomic number 54) was first recognized by Winkler and Spira [1] in 1966. Unlike iodine, xenon is highly lipid-soluble, and therefore it is a diffusible indicator that freely crosses the blood-brain barrier. Early reports on the use of stable xenon as a contrast agent for CT began with Haughton et al. [2] in 1976, and a year later Winkler et al. [3] suggested its potential utility as an indicator of cerebral blood flow (CBF). In 1978 Kelcz et al. [4] defined the blood-brain partition coefficient, and Drayer et al. [5] reported the first CBF measurements using the stable xenon CT technique. General Electric incorporated the technique with their 9800 series in 1983, and since that time Picker, Philips, Toshiba, Siemens, and other independent companies have developed either integrated or freestanding systems. The stable xenon CT CBF technology has been slow to be accepted, in part owing to the concerns of the pharmacologic properties of xenon, as well as to the labor-intensive nature of the examination. Despite these difficulties, clinicians who need rapid access to quantitative CBF information about their patients are showing an increasing interest in this technology.

Cerebrovascular Physiology

The maintenance of a disproportionately large and constant blood supply to the brain is essential because of the brain's high metabolic demand and its inability to store energy. Multiple mechanisms contribute to maintaining this blood supply. Global and regional CBF (reflecting both gray and white matter compartments) is about 50–55 ml per 100 g of brain tissue/min (50–55 ml · 100 g^{-1} · min^{-1}) in the adult, with significantly higher values in those below 20 years of age and a decrease in those over 60 years.

Received October 16, 1990; accepted without revision October 23, 1990.

[1] Department of Radiology, University of Pittsburgh School of Medicine, Presbyterian University Hospital, Pittsburgh, PA 15213. Address reprint requests to D. W. Johnson.
[2] Department of Radiology, Medical College of Virginia, Box 615 MCV Station, Richmond, VA 23298.
[3] Department of Diagnostic Radiology and Nuclear Medicine, S072, Stanford University School of Medicine, Stanford, CA 94305.
[4] Departments of Neurosurgery and Radiology, University of Pittsburgh School of Medicine, Montefiore Hospital, 3459 Fifth Ave., Pittsburgh, PA 15213.
[5] Department of Radiology, University of Pittsburgh School of Medicine, RC508 Scaife Hall, Pittsburgh, PA 15261.

While an increase in oxygen saturation has a modest inverse effect on CBF, carbon dioxide tension (Pco_2) has a potent direct effect, causing a 3–5% increase in CBF per mm Hg increase in carbon dioxide (CO_2) within the range of 20–60 mm Hg in normal individuals [6]. Although global blood flow tends to be fairly stable, local flow varies directly with local brain function by 10–20%. Extremes of metabolic activity such as those that occur in epilepsy or coma are accompanied by localized or global elevation or depression of CBF by 30–40%. Deep white matter or thalamic injury will result in a 20–30% ipsilateral reduction in cortical blood flow and an associated reduction of metabolic activity of the overlying cortex due to deafferentation [7].

Under normal conditions, change in cerebral perfusion pressure between 50 and 130 mm Hg produces little change in CBF [8–10]. Constant flow is maintained primarily by varying precapillary resistance. This ability to maintain a constant CBF over a wide physiologic range of arterial blood pressure is termed autoregulation. Below about 40 mm Hg, CBF will drop linearly with a drop in blood pressure because vasodilatation is maximal. Above 140 mm Hg, CBF will rise because vasoconstriction is maximal (Fig. 1). Autoregulation can be impaired in a variety of disease states such as vasospasm secondary to subarachnoid hemorrhage, head trauma, diffuse hypoxia, and focal fixed ischemic disease or embolism. In these situations, CBF will vary directly with blood pressure.

An absence of blood flow is rapidly accompanied by the cessation of metabolism, which, if allowed to persist for more than a few minutes, results in infarction, and a duration severity relationship between reversible ischemia and infarction is well established [11].

Oxygen delivery to the brain normally far exceeds demand. When autoregulatory limits are exceeded during arterial hypotension (vasodilatation is maximal), CBF falls and oxygen extraction from the blood increases. This state has been termed misery perfusion [12]. When this mechanism is exhausted, cellular metabolism is depressed. Neuronal function ceases, although the neurons may remain viable and recover function if perfusion is restored. For such transient ischemic events to occur, CBF must fall below the ischemic threshold of about 20 ml · 100 g^{-1} · min^{-1} for gray matter but must remain above the infarct threshold of about 15 ml · 100 g^{-1} · min^{-1}.

Thus, CBF methodologies that are rapidly repeatable and quantitative should be able to test for misery perfusion by altering blood pressure or acid-base balance. The diagnosis of this preclinical state is important because it permits clinical intervention prior to an irreversible injury. In acute stroke (less than 4–6 hr), quantitative flow information should be clinically relevant.

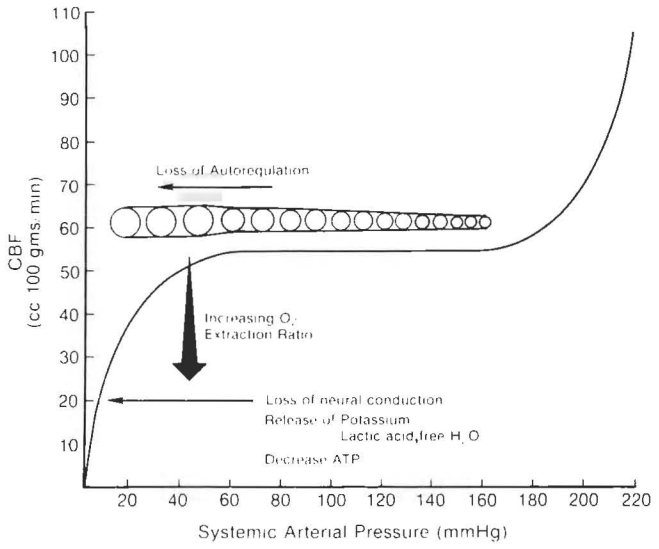

Fig. 1.—Cerebral blood flow (CBF) as a function of systemic arterial pressure. Maintenance of a constant CBF over a wide range of systemic arterial pressures is made possible by varying vessel caliber. Maximal vasoconstriction with precipitous rise in CBF occurs above 160 mm Hg. Maximal vasodilatation with precipitous drop in CBF and increasing oxygen (O_2) extraction occurs below 40–50 mm Hg. ATP = adenosine triphosphate.

Experimental and Clinical Use of Xenon CT CBF

The xenon CT CBF technique has been validated in animal studies and is currently being used clinically in the diagnosis of acute stroke, occlusive vascular disease, carotid occlusion testing, vasospasm, arteriovenous malformations (AVMs), and head trauma. This section provides a short review of the work that has been done in both the laboratory and clinical areas; then, the technical aspects of the technique are described, followed by a discussion of its advantages and disadvantages.

Correlation Studies and Laboratory Validation

Studies that correlate the xenon CT CBF technique to the radiolabeled microsphere technique in baboons have shown a high degree of correlation over a wide range of flows [13–15].

Wolfson et al. [16] compared stable xenon CT and ^{14}C-iodoantipyrine CBF measurement in baboons at severely reduced blood pressure and observed a correlation coefficient of .92 at CBF levels of 5–10 ml · 100 g^{-1} · min^{-1}.

In a baboon model of acute focal cerebral ischemia following lateral striate artery occlusion, flow values of less than 5 ml · 100 g^{-1} · min^{-1} were repeatedly recorded within the ipsilateral caudate and putamen and always led to infarction if duration of occlusion was greater than 1 hr [17]. In another baboon study, acute reperfusion of infarcted tissues resulted in an absolute hyperemia that persisted for more than 3 hr and was accompanied by low density on CT (Fig. 2) [18].

Normative Human Data

Mixed cortical flows of 67 volunteers ranging in age from 22 to 78 years averaged 51 ± 10 ml · 100 g^{-1} · min^{-1} using the xenon CT CBF method (Yonas H and Darby JM, unpublished data). High- (gray matter) and low- (white matter) flow compartment averages were 84 ± 14 and 20 ± 5 ml · 100 g^{-1} · min^{-1}, respectively. There was a significant decline with age in the high-flow compartment. These findings correlate well with other techniques [19–21].

Stroke and the Impact of Measuring Zero Flow

Xenon CT CBF values less than 12 ml · 100 g^{-1} · min^{-1} in gray matter invariably result in infarction (Fig. 3) [22, 23], while flows greater than 15 ml · 100 g^{-1} · min^{-1} may be compatible with recovery [23] (Stringer WA et al., unpublished data). This correlates well with positron emission tomography [24] and ^{133}Xe methods [11]. Furthermore, the identification of flow values near zero in all areas of selected slices has invariably been correlated with brain death of the individual (Fig. 4) [25–27] (Pistoia F et al., unpublished data).

Quantitative information has important implications in

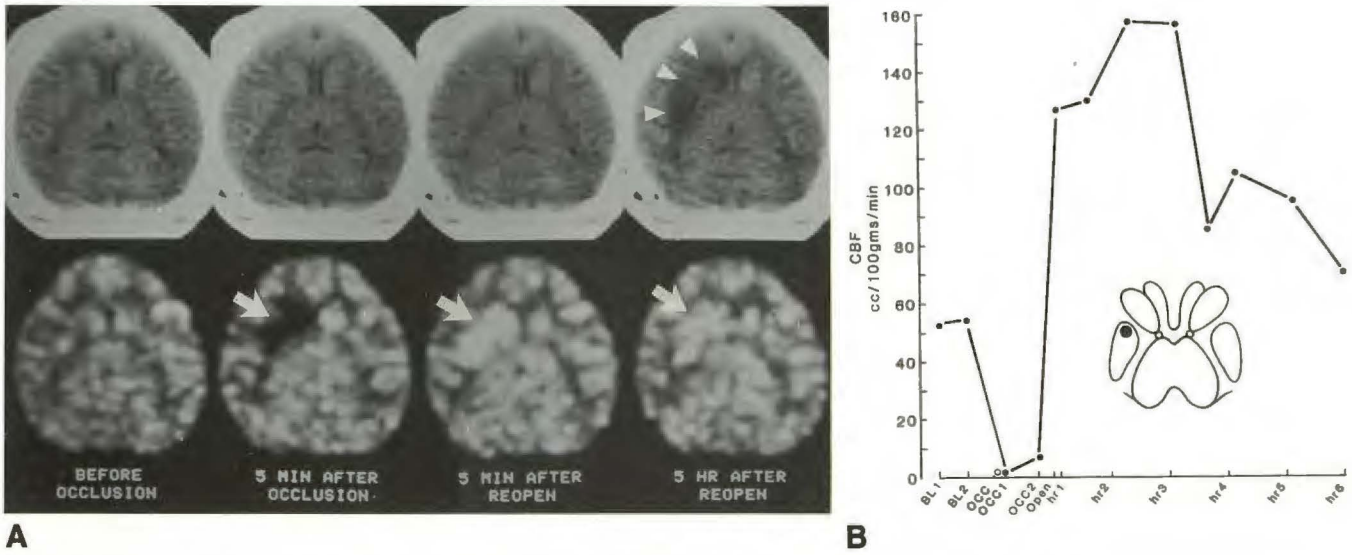

Fig. 2.—Xenon CT enhanced study of a baboon before, during, and at two intervals after 60-min occlusion of right lateral striate artery.

***A*, CT images (top row) and accompanying cerebral blood flow (CBF) maps (bottom row). Note absence of flow on CBF map in right basal ganglia at 5 min after occlusion (*arrow*). Reperfusion of territory results in hyperemia at 5 min after reopening of occluded artery (*arrow*). By 5 hr, CBF begins to fall to baseline levels (*arrow*). CT now shows infarct (*arrowheads*).**

***B*, CBF in right lentiform nucleus as a function of time. Schematic drawing represents basal ganglia; black dot in right lentiform nucleus represents location of region of interest. Note absolute hyperemia following reperfusion of infarcted territory. OCC = occlusion.**

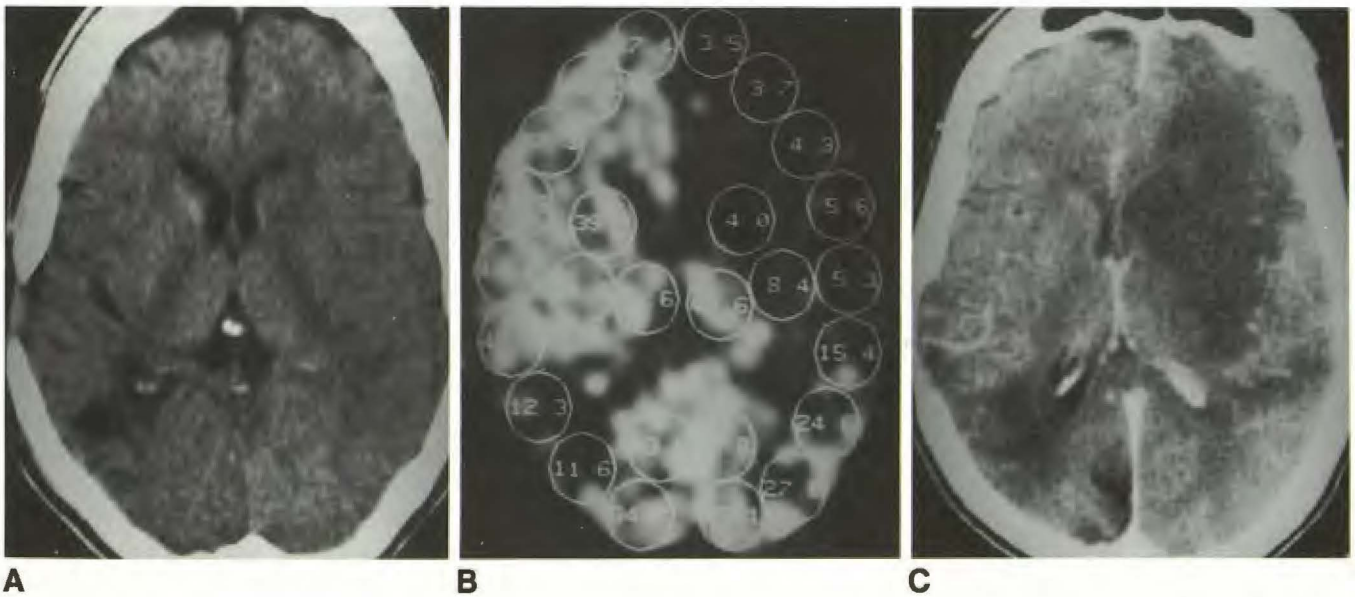

Fig. 3.—66-year-old woman with sudden onset of right hemiplegia in recovery room following a left carotid endarterectomy for high-grade stenosis of the internal carotid artery.

***A*, Baseline CT scan shows old infarct in right parietal lobe and subtle sulcal effacement in territory of left middle cerebral artery.**

***B*, Xenon CT cerebral blood flow study shows flows of 3–8 ml · 100 g^{-1} · min^{-1} in distributions of left anterior cerebral artery and anterior middle cerebral artery. In distributions of right anterior cerebral artery and anterior middle cerebral artery, flows average 45 ml · 100 g^{-1} · min^{-1}.**

C, CT study 3 days later shows a large infarction in left hemisphere corresponding to low flows on prior cerebral blood flow study.

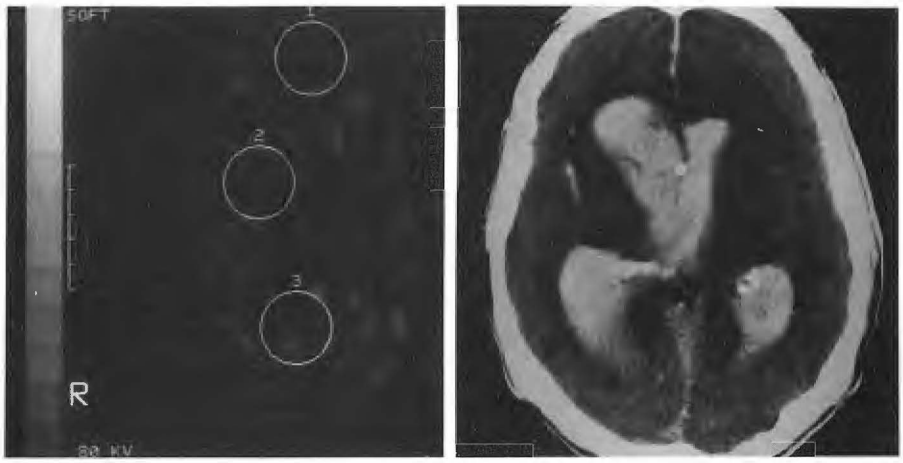

Fig. 4.—74-year-old man who fell off a stool and never regained consciousness. Over the next 24 hr, all brainstem reflexes were lost.

***A*, Xenon CT cerebral blood flow study revealed flows of 1.1, 2.3, and 2.9 ml · 100 g^{-1} · min^{-1} in regions of interest 1, 2, and 3, respectively. Gray-scale range of 0–100 ml · 100 g^{-1} · min^{-1} is supplied. Flows at two other levels (*not shown*) were similar.**

***B*, Accompanying CT scan shows massive intraventricular hemorrhage and loss of normal gray-white distinction.**

stroke therapy, for some therapies can have undesirable side effects. Calcium channel blockers can induce hypotension and increase the likelihood of infarction. Flow augmentation techniques such as hypervolemia, hemodilution, and induced hypertension may compromise the cardiopulmonary status of the elderly patient. Thrombolytic therapy is associated with the risk of converting a bland infarction to a hemorrhagic one [28, 29] and should be avoided if efforts to reperfuse are limited to tissues not irreversibly infarcted. In extreme cases, life-threatening mass effect might surgically be removed only if the tissue is known to be irreversibly infarcted.

"Luxury" perfusion, that is, perfusion in excess of metabolic requirements within injured tissues, may occur with reperfusion of an infarct or via collateral circulation at its periphery. Acute reperfusion of severely ischemic tissues is accompanied by absolute hyperemia (values greater than 70 ml · 100 g^{-1} · min^{-1}) that may last for 4–8 hr [30]. During the later phases of infarct evolution, however, a relative hyperemia with flow values that are low but greater than necessary for metabolism is commonly seen, and in these cases CBF information alone cannot provide insight about the viability of tissue. The coupling of CT changes aided by definition of blood-brain barrier alteration as indicated by iodine entry into tissue, however, can help define the true nature of even this injury. It may also be accompanied by other evidence of metabolic derangements such as a severely abnormal electroencephalogram (Stringer WA et al., unpublished data).

The very complexity of cerebrovascular physiology suggests that no one therapy is likely to be effective in all cases of acute cerebral ischemia. Therefore, identification of the baseline pathophysiology is necessary to determine which forms of treatment have a reasonable chance of success in a given situation, a concept we believe is important to the design of future stroke therapy trials.

Clinical Challenge Studies

CBF is dependent on many variables, for example, blood pressure, age, rheology, prior injury, and local or generalized brain metabolic activity; thus, a single CBF study with low mixed cortical flows but above the ischemic threshold of 20 ml · 100 g^{-1} · min^{-1} is of relatively little use in understanding if a region is at increased ischemic risk. Reduced flows may be due to either low supply or low demand. Therefore, to determine if a region is at increased hemodynamic risk, CBF methodology must be repeatable after a short interval in order that flow alterations, if any, that occur in response to a physiologic challenge can be assessed. It must be capable of providing a challenge to collateral flow (if the primary supply is interrupted), autoregulatory status, or response to CO_2.

Balloon Test Occlusion of the Internal Carotid Artery

The treatment of aneurysms, fistulas, and tumors encasing the carotid artery may require temporary or permanent occlusion. The Matas test (external compression of the common carotid artery) was the approach used for years to clinically assess the safety of permanent occlusion of the carotid artery. Temporary endovascular balloon occlusion of the internal carotid artery and CBF measurement is an invasive refinement of the Matas test [31, 32]. In this procedure, if the patient passes 15 min of test occlusion, he or she is then transported to the CT scanner with the balloon deflated (but in the internal carotid artery), where a CBF study is performed with the balloon inflated. In 12% of a group of 136 patients, a significant ipsilateral reduction of CBF was found that was not identified by clinical testing alone [32]. Balloon occlusion stump pressures, however, were not predictive of marginal CBF. In this group no cerebral perfusion reserve remains, and the patient is presumed to be at high risk for stroke should even mild hypotension occur. One such patient had surgical resection of the internal carotid artery without protective measures and suffered a stroke in those territories that, by balloon occlusion testing, dropped near the ischemic threshold (Fig. 5). Furthermore, 21 consecutive patients in whom normal balloon occlusion flows were demonstrated underwent permanent carotid occlusion without stroke [32]. The surgeons at the University of Pittsburgh now make extreme

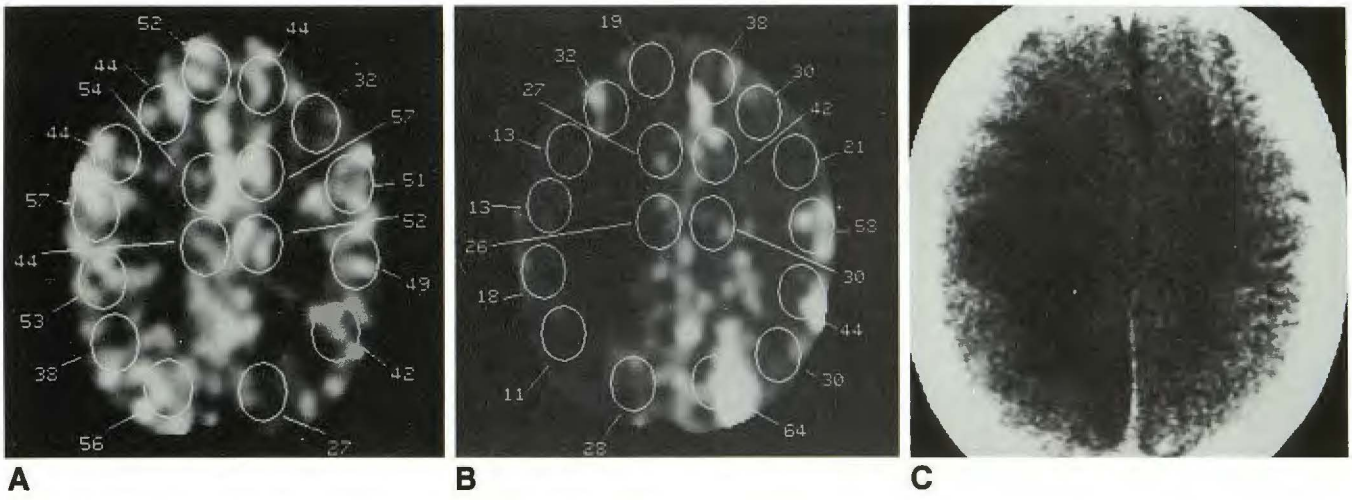

Fig. 5.—58-year-old man with squamous cell carcinoma of right skull base. (Erba group III.)
***A*, Baseline unoccluded study shows cerebral blood flow values.**
***B*, Balloon test occlusion of right internal carotid artery. Patient passed the clinical portion of the study but there was significantly decreased flow in right hemisphere.**
***C*, During surgery the carotid artery was sacrificed without graft placement, resulting in a large infarct.**
(Reprinted from Erba et al. [31].)

efforts to improve collateral flow prior to or during internal carotid occlusions in the marginal collateral flow group.

Acetazolamide Challenge of Reserve in Occlusive Vascular Disease

First described by Vorstrup et al. [33], the acetazolamide (Diamox, Lederle) challenge of vascular reserve appears to have important diagnostic implications in patients with occlusive vascular disease. Acetazolamide, 1–2 g IV, leads to maximal vasodilatation of cerebral vasculature within 10–20 min, presumably by inhibiting carbonic anhydrase and causing local retention of hydrogen ions. Acetazolamide challenge of cerebrovascular reserve studied with xenon CT was first described by Rogg et al. [34] in 1989; they found that only 24% of patients with severe occlusive vascular disease had significant reserve compromise. In these patients, acetazolamide challenge either caused no change in or actually lowered CBF from the baseline levels. Reserve compromise patterns may be global, but often correlate closely with one or two arterial territories or may be detected in the watershed border-zone territories at the convexities. Two-year follow-up in 24 patients with compromised reserved, as defined by xenon CT CBF, showed a 55% prevalence of transient ischemic attacks and 23% prevalence of new cerebrovascular accidents [35]. This evidence suggests that these individuals are at increased risk of stroke (Fig. 6). Cerebral vasoreactivity is reported to improve following extracranial-intracranial bypass [36].

Autoregulation and Reserve Testing in Vasospasm

Angiographic vasospasm occurs in 40–80% of patients after subarachnoid hemorrhage, but in only 20% of patients do flow values fall low enough to produce ischemic symptoms. At the University of Pittsburgh, in every case of delayed neurologic deficit due to angiographically defined vasospasm, we have observed flow values at or below 25 ml · 100 g^{-1} · min^{-1}, as noted by Symon [37]. Flow in this range of 20–30 ml · 100 g^{-1} · min^{-1} is associated with mild reversible deficits. Flows less than 15 ml · 100 g^{-1} · min^{-1}, also noted by Powers et al. [24], are associated with irreversible fixed deficits and CT-defined infarctions [38]. In contrast to other reports in the literature, CBF can in fact fall abruptly from normal to near zero within hours (Fig. 7) and severe ischemia can occur remote from the vessel of aneurysm origin.

Xenon CT CBF data have shown better correlation with deficits and CT-defined infarction than has transcranial Doppler, which is insensitive to second-order vessel spasm. Because symptomatic vasospasm is due to constriction of the conductance vessel and is associated with maximal vasodilatation distally, normal autoregulation is lost and distal tissue perfusion is directly dependent on blood pressure. In this situation CBF studies have shown that the elevation of systemic blood pressure with dopamine can be shown to elevate critically low blood flow, but dopamine can lower CBF to levels as low as 15–20 ml · 100 g^{-1} · min^{-1}. In these individuals dopamine therapy is potentially harmful. This probably represents a return to normal autoregulation and an indication to discontinue therapy. The prolonged use of hypertension and hemodilution in the treatment of vasospasm can compromise the cardiac status of the elderly patient [39]. CBF response to Pco_2 variation also has been valuable for assessing cerebrovascular reserve in these patients [40]. The ability to evaluate autoregulation and cerebrovascular reserve directly with xenon CT CBF has limited aggressive hypertensive therapy for vasospasm at the University of Pittsburgh to less than 5% of post–subarachnoid hemorrhage patients (Fig. 8).

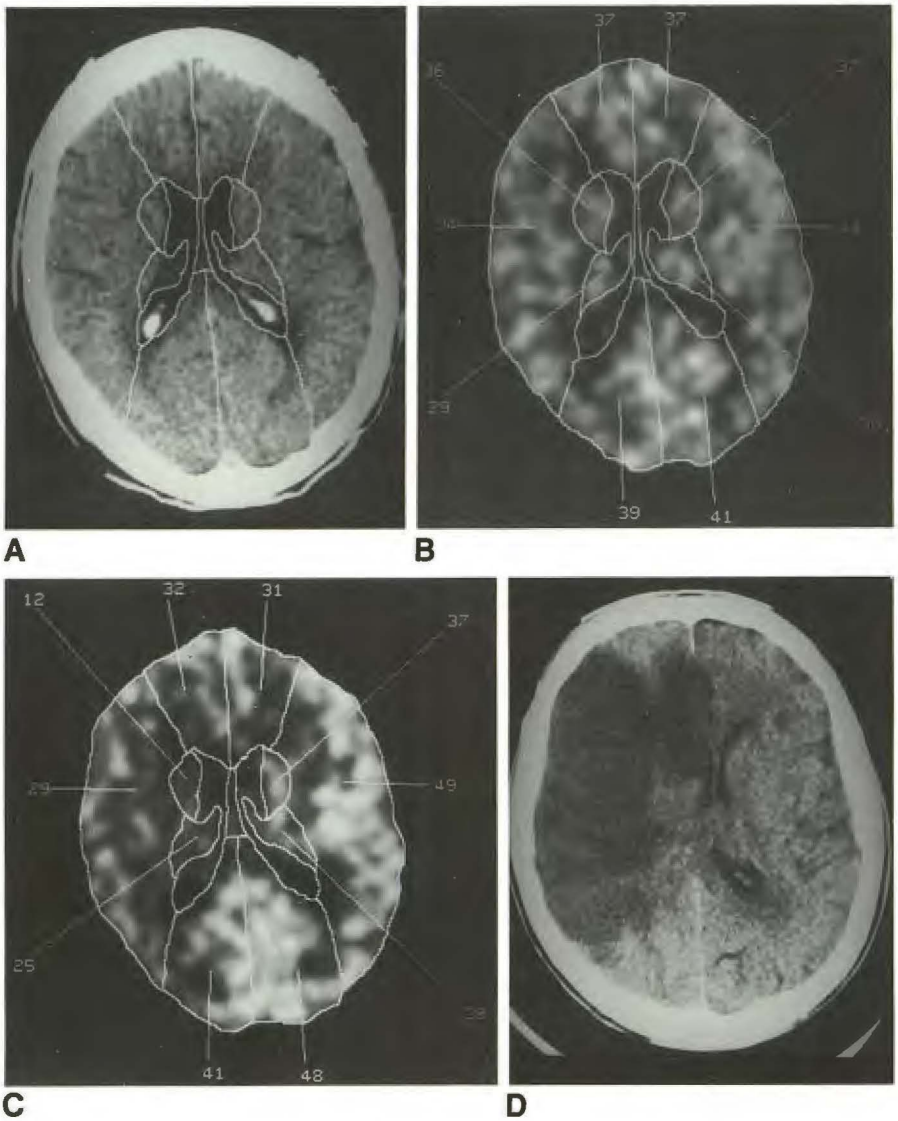

Fig. 6.—Acetazolamide challenge in a 55-year-old man with symptomatic vascular occlusive disease. Angiography showed occlusion of left internal carotid artery (ICA), 95% stenosis of right ICA with collaterals from left external carotid artery, posterior circulation, and right ICA filling left ICA branches.

***A*, Baseline CT scan at level of lateral ventricles with regions of interest supplied.**

***B*, Pre-Diamox study with cerebral blood flow (CBF) values supplied.**

C, Post-Diamox study shows flow reduction in territories of right middle and both anterior cerebral arteries. Augmentation of flow is seen elsewhere.

***D*, Surgery was scheduled, but 36 hr after the study a sudden stroke occurred in those territories predicted to be at risk by CBF study.**

(Reprinted from Rogg et al. [34].)

Vascular Steal Phenomenon in AVMs

AVMs are composed of low-resistance vascular channels. The phenomenon of steal occurs when blood is shunted through the low-resistance AVM away from the higher-resistance capillary bed in the surrounding brain. Many of the symptoms patients with AVMs develop, including seizures, progressive neurologic deficits, and intellectual or emotional deterioration, have been attributed to steal.

It is difficult to prove that a patient's symptoms are caused by reduced flow to regions of the brain surrounding the AVM. Regional CBF measurements have been performed to evaluate changes in flow that result from the altered hemodynamics produced by the AVM. Homan et al. [41] used ^{133}Xe single-photon emission CT and demonstrated areas of flow reduction that were located randomly in the hemispheres both contralateral and ipsilateral to the AVM. Okabe et al. [42] observed CBF values to be significantly reduced adjacent to the AVM when compared with those in similar regions in age-matched normals. This study also found improvement in flow after excision. Marks et al. [43] used xenon CT to compare CBF in cortical regions of interest (ROIs) in ipsilateral and contralateral hemispheres. Compared with the contralateral hemisphere, statistically lower flows were found in cortices adjacent to the AVM as well as in ipsilateral cortices predicted by angiography to have reduced flow. Similar ROIs were measured in a group of AVM patients with steal symptoms and compared with AVM patients without steal [44]. AVM patients with steal were more likely to have regions of decreased flow (<30 ml $\cdot$ 100 $g^{-1} \cdot min^{-1}$) and more profound mean differences between contralateral and ipsilateral hemispheres. However, the mean differences were not statistically significant when comparing steal and nonsteal patients.

Acetazolamide challenge has also been used to evaluate flow in the AVM patient. Tarr et al. [45] have used xenon CT in conjunction with acetazolamide challenge and identified two abnormal patterns of flow response. Several patients exhibited low baseline CBF and normal augmentation with

Fig. 7.—24-year-old man with subarachnoid hemorrhage from an anterior communicating artery aneurysm.

***A*, Initial xenon CT cerebral blood flow (CBF) map (left) shows no critically low flows and patient underwent surgery. Corresponding CT image (right).**

***B*, 24 hr after aneurysm clipping, left-sided weakness developed, greater in the leg than in the arm. CBF study (left) shows flows of 5 ml · 100 g^{-1} · min^{-1} in territory of right anterior cerebral artery (ACA) (*solid arrows*) and 20 ml · 100 g^{-1} · min^{-1} in left ACA territory (*open arrows*). CT study (right) is normal.**

C, 6 days after aggressive treatment with hypertension, flows in left ACA improved (*open arrows*), but flows on right (*solid arrows*) did not.

***D*, CT scan 2 years later shows only right ACA infarct.**

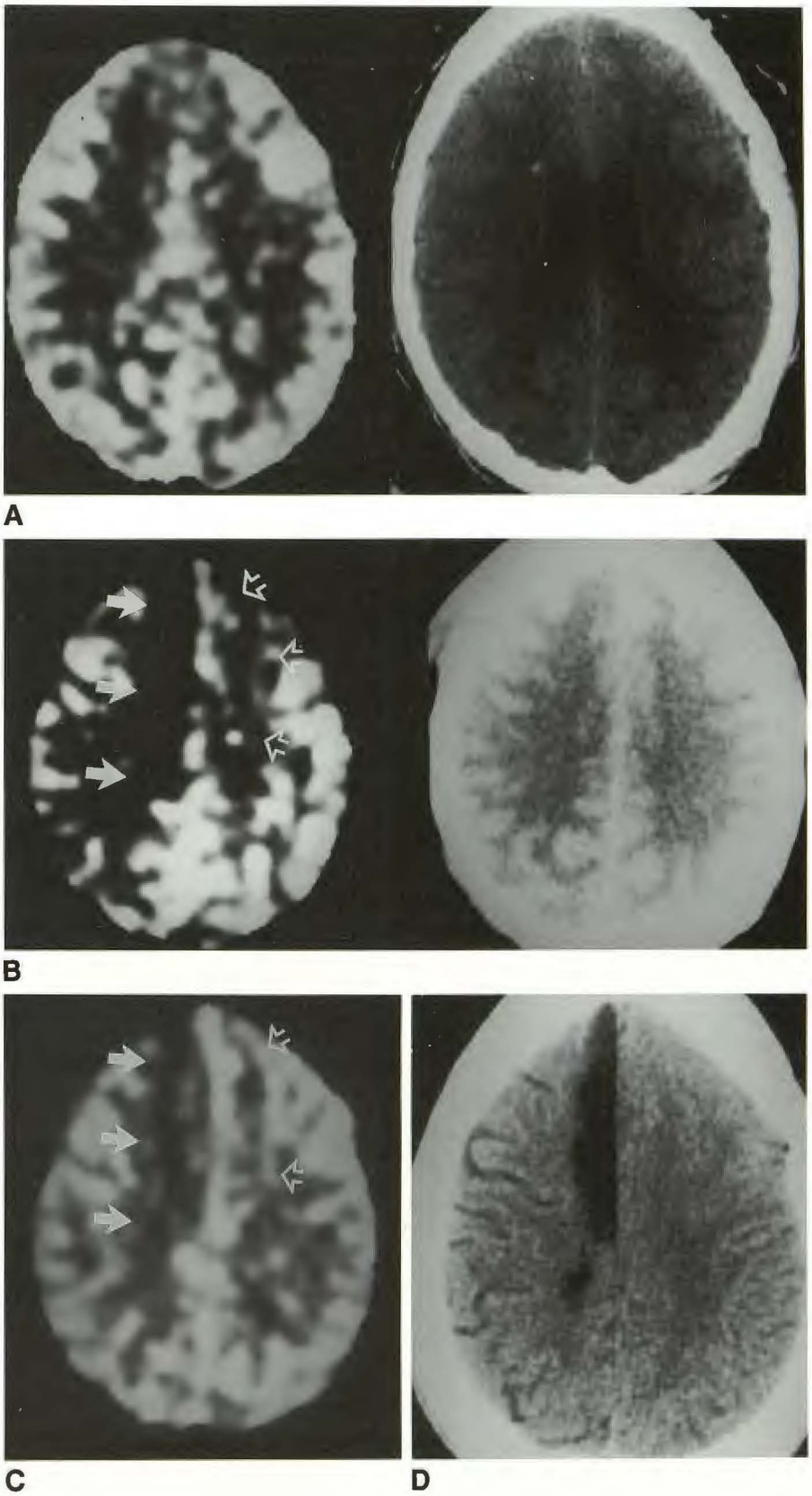

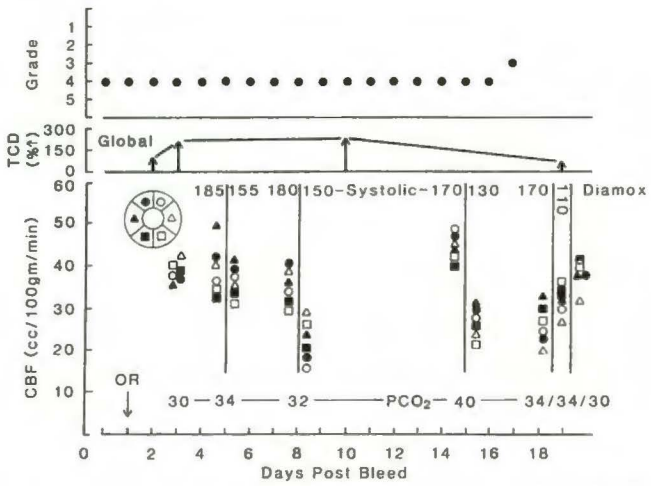

Fig. 8.—Graph depicting postoperative course in a 69-year-old woman with posterior communicating artery aneurysm. The patient underwent surgery (OR) 1 day after subarachnoid hemorrhage. Because transcranial Doppler (TCD) indicated increased velocities, xenon CT cerebral blood flow (CBF) blood pressure (BP) challenge study was done on day 5 at systolic pressures of 185 and 155 mm Hg. Each of six brain regions (three major vascular territories on each side) are depicted schematically by the pie symbol on left. Because no change in CBF was seen, hypertensive therapy was postponed until another blood pressure challenge study on day 8 showed direct dependence of CBF on level of blood pressure. Similar findings were seen again on day 15. Transcranial Doppler revealed a drop in velocities on day 19. CBF was paradoxically lower at the elevated systolic blood pressure level of 170 mm Hg. Dopamine was stopped and systolic pressure dropped to 110 mm Hg. CBF increased slightly. Diamox was also given, showing further augmentation of CBF. (Reprinted with permission from Yonas [40].)

acetazolamide. Others had a normal or low baseline CBF but had areas of decreased augmentation (Fig. 9). AVM patients with lowered augmentation or diminished vascular reserve may represent an important subgroup because they exhibit arterial regions that are maximally dilated and unable to respond to acetazolamide. These patients may be at higher risk for normal-perfusion breakthrough bleeding at surgical resection or during embolization. However, one report has suggested that increased augmentation rather than decreased augmentation may occur in patients prone to normal-perfusion breakthrough bleeding [46]. Further clinical studies are needed to assess flow-related changes in patients who may be at risk for this catastrophic complication.

Head Trauma Management

Ischemic brain damage is common in patients who die of head injury [47]. Several investigators have observed low CBF in the first few hours after injury [48–52]. Yet hyperemia also can be commonly observed in the hours to days that follow [53–56], and its relationship to elevated intracranial pressure (ICP) and decreased cerebral perfusion pressure [57] has led to the rationale of hyperventilation as a method of controlling elevated ICP [54, 58]. Beyond control of ICP, hyperventilation is believed to be beneficial in controlling CSF acidosis [59]. Ward et al. [60], however, recently reported a poorer outcome in a group of patients with severe head injury who were prophylactically hyperventilated vs a control group that was not hyperventilated. Assuming an intact vasoreactivity of 3–5% change in CBF per mm Hg change in CO_2, one might be able to lower CBF predictably; however, vasoreactivity after head injury is not a predictable 3–5%/mm Hg (Fig. 10) [61, 62], and the "inverse steal" phenomenon (the shunting of blood from normal tissue with intact vasomotor reactivity to damaged tissue that has lost vasomotor reactivity) has been observed (Fig. 11) [61, 63]. Furthermore, there are local differences in CBF and vasoreactivity in sharply defined cortical regions and in deep structures that may not be appreciated by nontomographic techniques [63, 64] (Marion DW et al., unpublished data). The poorer outcome in the hyperventilated group that Ward et al. [60] reported might well be due to infarction of marginally perfused areas of normal brain tissue.

One cannot predictably alter CBF by altering P_{CO_2}, and xenon CT CBF can identify those patients at risk for ischemia who are being hyperventilated for control of ICP. Therapy to control ICP must be balanced with the need to maintain adequate CBF.

Technique

CBF Calculation and Measurement

Like other methods that indirectly measure CBF, the stable xenon technique uses Kety's application of the Fick principle of indicator dilution, which relates the concentration of a freely diffusible nonmetabolized indicator absorbed in the tissue per unit time as the difference between the arterial and venous concentrations of the indicator [65]. In the case of stable xenon gas, the gas's radiodensity allows its concentration in the brain to be determined directly by the CT scanner, so that measurement of the venous concentration is unnecessary. Conceptually, the brain xenon concentration is related to the arterial concentration of xenon (which is itself time-dependent), the brain blood flow, and the duration of exposure to xenon (since the equilibration of xenon between brain and blood is not instantaneous). These factors determine the total amount of xenon presented to the brain. Uptake is also determined by the affinity of the brain for xenon, which is measured by the brain-blood partition coefficient, lambda (λ). This reflects the relative solubility of xenon gas in the brain and blood or, more simply, the xenon concentration in the brain and blood at equilibrium. These factors are related mathematically by the Kety-Schmidt equations modified for the xenon CT technique:

$$CXe_{Br}(t) = \lambda k \int_0^t CXe_{Art}(u)\, e^{-k(t-u)}\, du \qquad (1)$$

and

$$F = \lambda k, \qquad (2)$$

where $CXe_{Br}(t)$ = time-dependent brain xenon concentration, λ = brain:blood partition coefficient, k = brain uptake flow rate constant, $CXe_{Art}(u)$ = time-dependent arterial xenon concentration, and F = CBF.

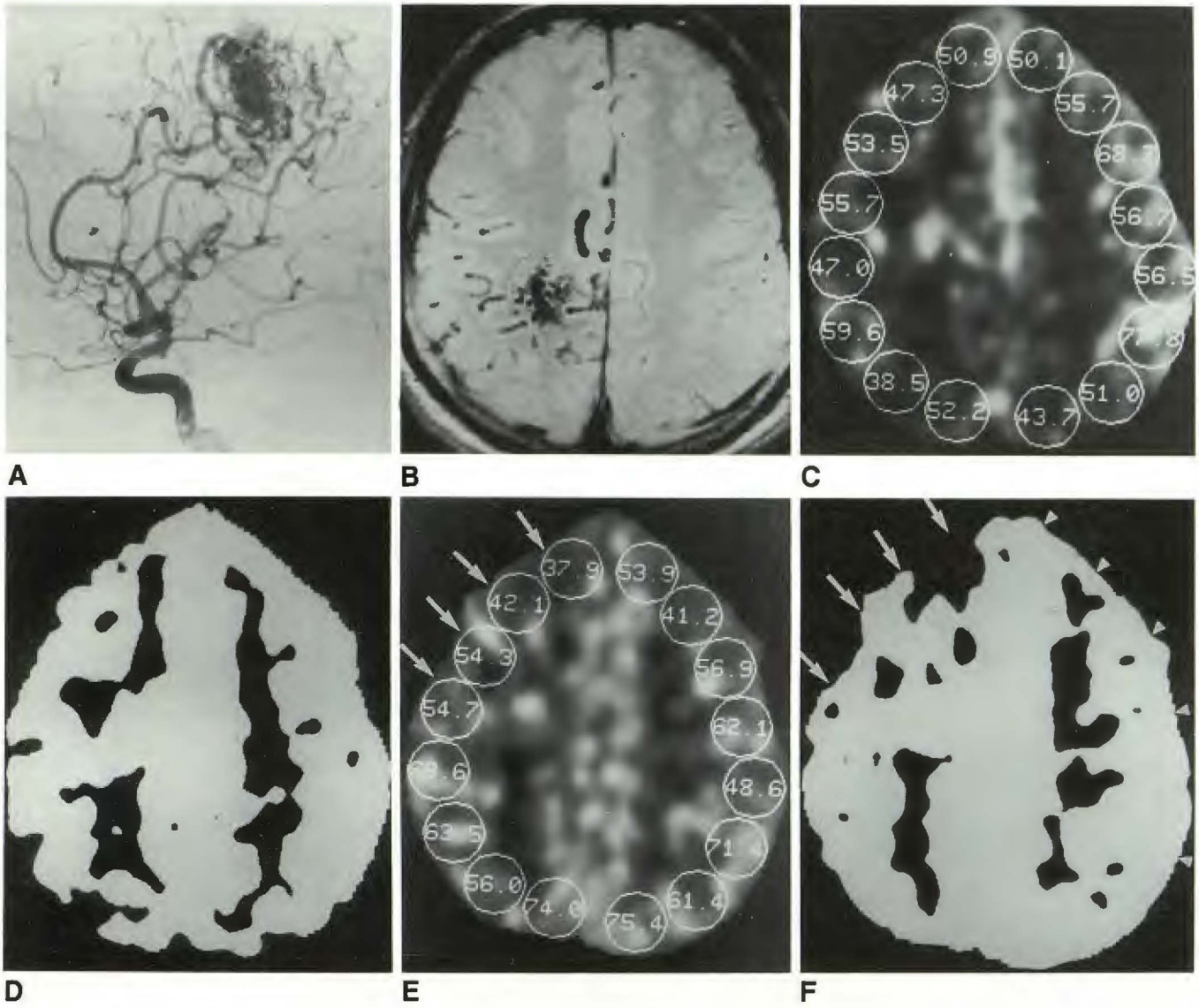

Fig. 9.—20-year-old man with intractable seizures.

***A*, Angiogram reveals pericallosal and middle cerebral arterial supply to parietal arteriovenous malformation (AVM).**

***B*, Axial MR image, 2000/20/1 (TR/TE/excitation), shows flow void in AVM in parietal centrum semiovale. No surrounding parenchymal abnormalities are seen.**

***C*, Pre-Diamox xenon CT cerebral blood flow (CBF) map, with values supplied, shows all flow values above 45 ml · 100 g^{-1} · min^{-1} except for parietal watershed border zones.**

***D*, Pre-Diamox xenon CT CBF contrast map of *C* (window level = 35; window width = 2). All flows above 35 ml · 100 g^{-1} · min^{-1} are white.**

***E*, Post-Diamox xenon CT CBF map, with values supplied, shows cortical regions both in near sites (*arrows* in *E* and *F*) and sites distant from AVM (*arrowheads* in *F*) that fail to show normal augmentation of CBF. These regions represent decreased vascular reserve.**

***F*, Post-Diamox xenon CT CBF contrast map of *E* (window level = 35; window width = 2) shows fewer pixels in frontal regions with flows above 35 ml · 100 g^{-1} · min^{-1}.**

(Reprinted from Tarr et al. [45].)

Time-dependent arterial xenon build-up is described by:

$$CXe_{Art}\ (u) = CXe_{max}\ (1 - e^{-bu}) \qquad (3)$$

where CXe_{max} = maximum arterial xenon concentration in mg/ml, u = time, and b = arterial uptake rate constant.

In practice, arterial xenon uptake is not measured directly but rather by assuming instantaneous equilibrium with end-tidal pulmonary xenon concentration. This assumption is valid in the absence of severe pulmonary disease or right-to-left intrapulmonary or intracardiac shunts. Maximum arterial xenon uptake in mg/ml is related to maximum percent arterial uptake by:

$$CXe_{max} = C\ (\%)_{max}\ (5.15)\ (S_{Xe})\ (0.01) \qquad (4)$$

where $C(\%)_{max}$ = maximum percent xenon uptake, 5.15 = density of xenon in mg/ml at 37°C and 1 atm, and S_{Xe} =

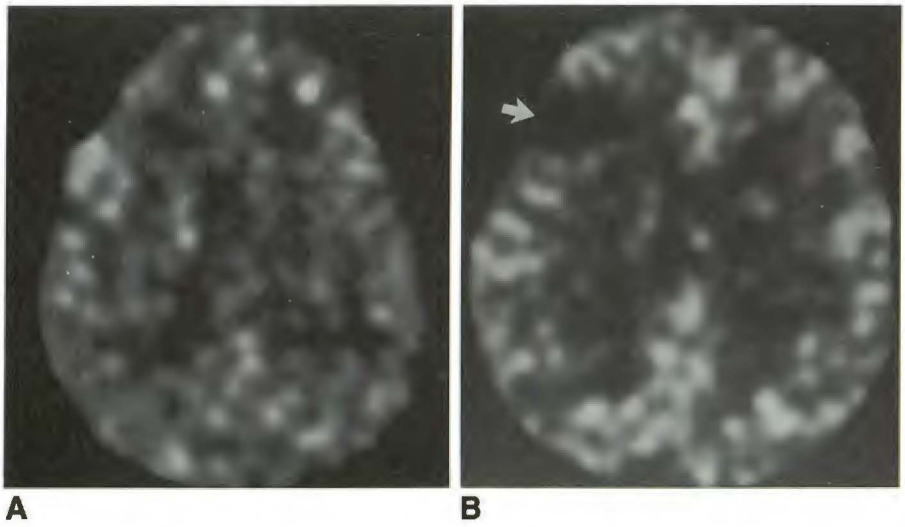

Fig. 10.—Range of cerebral blood flow (CBF) values encountered for a given carbon dioxide tension (Pco_2) level in head trauma can be extreme.

A, Xenon CT CBF study in an 85-year-old woman at a Pco_2 of 23 mm Hg has a global flow of 18 ml · 100 g^{-1} · min^{-1}. Other than a slight residual mass effect following a subdural hematoma evacuation there was no CT abnormality.

B, Xenon CT CBF study of a 33-year-old man at a Pco_2 of 21 mm Hg has a global flow of 46 ml · 100 g^{-1} · min^{-1}. CT image showed only a contusion in right frontal cortex corresponding to absent flow seen on blood flow map (*arrow*).

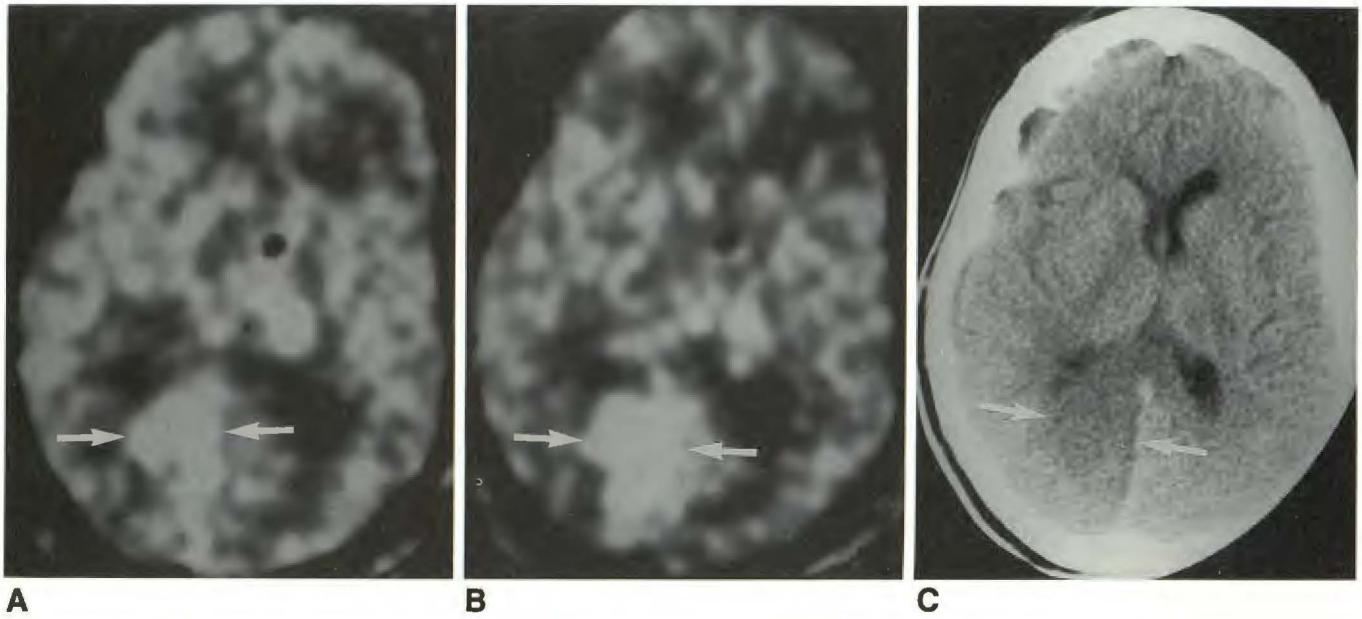

Fig. 11.—15-year-old girl with severe head trauma demonstrating "inverse steal" phenomenon in right calcarine cortex.

A, At a carbon dioxide tension (Pco_2) of 32 mm Hg, flow in right calcarine cortex is 57 ml · 100 g^{-1} · min^{-1} (*arrows*); elsewhere, flows are 68 ml · 100 g^{-1} · min^{-1}.

B, At a Pco_2 of 23 mm Hg, flow in right calcarine cortex has increased to 108 ml · 100 g^{-1} · min^{-1} (*arrows*); elsewhere, flows decrease to an average of 54 ml · 100 g^{-1} · min^{-1}.

C, CT scan 10 days later shows right calcarine infarct (*arrows*). Response to Pco_2 in normal regions by CT is 2.8%/mm Hg, but a −5.3% paradoxic response is seen in tissue that later proves to be infarcted.

Ostwald solubility of xenon in blood, related to hematocrit (Hct) by:

$$S_{Xe} = 0.1 + 0.0011\ (\%Hct) \quad (5)$$

Finally, the Hounsfield enhancement (HE) resulting from xenon in the brain is related to the concentration in mg/ml by:

$$HE = CXe_{Br}/(u_p^w/u_p^{Xe}) \quad (6)$$

where u_p^w and u_p^{Xe} are the mass attenuation coefficients of water and xenon, respectively.

With current technology on the GE 9800 system, measurement of xenon build-up in tissue is obtained in the following manner: Two baseline scans are obtained at two to three different levels before xenon inhalation. Three to six enhanced scans per level are then obtained during a 4.5-min xenon inhalation. The baseline scan pairs are averaged and then subtracted from each of the enhancement images to obtain $CXe_{Br}(t)$ for each of the 10,000–30,000 voxels in each image. A thermoconductivity analyzer measures end-tidal xenon concentration. This inexpensive device approaches the accuracy of a mass spectrometer [66].

With the relationships described above, the brain uptake data are fitted to Kety-Schmidt equation (equation 1) by using

an iterative least-squares approach. The two unknown parameters, flow (F) and lambda (λ), are simultaneously derived from the resulting curves for each voxel at each level. In this solution, errors of λ and k, tend to vary inversely so that mild variations in λ are compensated for by k, and the result is mathematically a very stable solution for blood flow. Noise between voxels is minimized by pre- and postcalculation smoothing routines.

The image that results is a map of CBF values with a full width at half maximum resolution of about 4 mm. Depiction of the CBF map will use a gray scale of 0–100 ml · 100 g^{-1} · min^{-1}. Numeric values of flow can be extracted by placing ROIs of any shape or size on the CBF map to obtain mean and standard deviations of flow. When large regions are measured, both gray and white matter are usually included in the ROI, and the flow measurement and standard deviation will reflect the averaging of these two compartments. Some manufacturers of xenon CT equipment provide lambda maps as well as flow maps in their display. These may allow for more accurate measurement of flow in "pure" gray matter by allowing pixels containing mostly CSF or white matter to be excluded from the measurement on the basis of their lambda value.

Owing to the inherent noise of the system, caution must be used in relying on numeric values from too small an ROI. Measurement accuracy rapidly improves as the number of included pixels increases, and it reaches an acceptable error of about 12% when the ROI is 1 cm^2 or larger, even in very low flow states. Thus, a value of 1.0 ± 1.0 ml · 100 g^{-1} · min^{-1} for the entire brain can be equated with flow at or very near zero with no statistically reasonable likelihood that there are flows compatible with tissue viability.

Signal-to-Noise Ratio vs Clinical Tolerance

The use of stable xenon as an indicator is not without limitations. While 80% xenon provides a high signal-to-noise ratio of 30:1, it is also a potent anesthetic agent at that concentration. At 50–60% concentration, xenon may cause sedation, and there is a high rate of bronchospasm and respiratory depression. In our experience with over 4000 examinations, more than half of which were performed in ambulatory outpatients, we have found that limiting the inhaled concentration of xenon to 33% (with 67% oxygen) provides a very acceptable level of clinical tolerance for 90% of patients [67], at the same time yielding an adequate level of signal to noise (about 8 to 1). Occasionally patients will exhibit some respiratory depression at these concentrations. Patients will almost always take a deep breath when asked to do so. Rarely, an examination is terminated prematurely because of prolonged respiratory delay. Improved signal-to-noise characteristics of CT scanners should permit a further reduction in xenon concentration.

Patient Preparation and Study Procedure

Adequate patient preparation and monitoring are essential to obtain a diagnostic study. Patient tolerance of sensory alterations is highly variable and seems to be dependent primarily on the individual's prestudy "mind set." Therefore, it is essential that each patient is briefed about the transient sensory disturbances that may occur during the examination. At the start of each study, the patient is wrapped with body restraints on the CT table in order to create a greater feeling of security. A modified head holder and a form-fitting evacuable "beanbag" (VacPac, Olympic Medical Supply Co., Seattle, WA) surround and limit motion of the head. The patient is instructed to respond to questions about his or her status during xenon inhalation with predetermined toe movements. During the examination the medical observer closely monitors and reassures the patient. These efforts are all important in limiting patient motion, because it is the most important factor determining the ultimate success of obtaining a diagnostic examination. Blood pressure, arterial oxygen saturation, end-tidal CO_2 concentration, and respiratory rate are continuously monitored during the study. Intubated patients are easily studied with xenon CT CBF, and nearly 100% of the studies yield diagnostic information.

Depending on the clinical indication for the particular study, two or three levels are then chosen. In the past, tube heat-loading constraints have limited the number of levels to be scanned, but new hardware and software systems will allow for more levels to be examined (Ansai & Yoygo Diversified Diagnostics). A face mask or mouthpiece (with nose clamp) is used to deliver the gas. If indicated, a second study is performed after 20 min, allowing time for adequate washout of xenon from the body tissues.

Advantages and Disadvantages of Xenon CT CBF

The main advantage of stable xenon CT is that it noninvasively provides relatively high-resolution, quantitative local CBF information coupled to CT anatomy. The information obtained is valid even in disease states because a partition coefficient is directly calculated for each voxel as small as 1 × 1 × 5 mm^3. CBF studies can be repeated at 20-min intervals, allowing for the evaluation of hemodynamic states as well as the response to therapeutic interventions. The technology can be incorporated within current CT technology at a cost lower than that of any dedicated tomographic CBF technology. Current reconstruction times also make the information available for review within a short enough interval so that therapeutic decisions can be made while the patient is still in the scanner.

The radiation dose, pharmacologic effects of xenon gas, and limitations of survey are three disadvantages of the xenon CT CBF technique that must be considered. In a two-level study that uses two baseline and six enhanced scans at each level (typically 80 kVp, 560 mAs), the absorbed dose to the center of the brain is approximately 8 cGy and 2 to 2.5 times higher to the skull. With current risk estimates, this amount of absorbed dose yields a lifetime risk of 1×10^{-4} to 1×10^{-5} that an average member of the population who undergoes this procedure will develop a radiation-related brain tumor. This risk decreases significantly for patients over the age of 50, or for those whose life expectancy is lower than that of the average member of the population. While the risk of this

procedure is generally considered to be at a clinically acceptable level and is considerably below that of angiography, the patient receives a dose of radiation that is not insignificant. When the procedure is performed, exposure of the relatively radiosensitive lens of the eye should be avoided.

The pharmacologic properties of xenon are associated with a number of theoretical and real problems. Xenon alters the sensorium of most individuals and may induce patient motion, but this can be minimized with careful prestudy positioning and reassurance of the patient during the study. While most find the sensation either more or less enjoyable, occasionally an individual cannot tolerate the perception of "losing control" and will demand to have the study stopped. For some, a small dose of fentanyl will minimize the anxiety they experience. While Winkler et al. [68] cautioned that 100% xenon can induce apnea, at 30%, xenon has been associated with a 3.6% prevalence of respiratory depression of greater than 10 sec [67].

Obrist et al. [69] observed a flow activation of 28% while human volunteers inhaled 30–35% stable xenon for 6 min. While flow activation, especially if early, could theoretically invalidate xenon as a tracer of CBF, several studies have indicated that because activation occurs after 2 min it has an insignificant effect on calculated flow [70] (Lindstrom WW, presented at the International Conference on Stable Xenon/CT CBF, February 1990; Good WF, unpublished data).

Should measurable flow activation occur there is a potential to induce an increase in ICP, but this has not been observed in one clinical and one animal study of ICP alterations during xenon inhalation in controlled ventilation (Darby J and Marion DW, separate papers presented at the International Conference on Stable Xenon/CT CBF, February 1990).

The study is currently limited to only two or three brain levels, but this is adequate when the goal is to evaluate large vascular territories. In the near future, contiguous level acquisition will become an option, but this will increase radiation exposure to the patient. A limited, but directed examination prompted by the baseline CT images can yield the most information with the smallest amount of radiation.

Beam-hardening artifacts continue to limit evaluation of the lower brainstem and cerebellum, but the upper brainstem and cerebellum are quite accessible with full gantry tilt and slight head flexion.

Conclusions

Xenon CT CBF imaging has a wide range of unique applications in acute clinical decision making; with slight modifications of standard CT technology, it is able to record very low flows. This method is inexpensive and offers anatomically coupled high resolution and repeatable quantification of CBF, allowing a variety of challenge studies to test cerebrovascular reserve and autoregulation. Future improvements will allow survey of more levels of the brain at a lower dose of radiation and inhaled xenon. Xenon CT will, however, continue to require close monitoring to ensure patient safety and minimize motion.

REFERENCES

1. Winkler SS, Spira J. Radiopacity of xenon under hyperbaric conditions. *AJR* **1966**;96:1035–1040
2. Haughton V, Harrington G, Schmidt J, et al. Xenon contrast enhancement for computed tomography scanning in multiple sclerosis. In: *Proceedings of international symposium on computer assisted tomography in nontumoral diseases of the brain, spinal cord and eye.* Bethesda, MD: National Institutes of Health, **1976**:
3. Winkler SS, Sackett JF, Holden JE, et al. Xenon inhalation as an adjunct to computerized tomography of the brain: preliminary study. *Invest Radiol* **1977**;12:15–18
4. Kelcz F, Hilal SK, Hartwell P, Joseph PM. Computed tomographic measurement of the xenon brain-blood partition coefficient and implications for regional blood flow: a preliminary report. *Radiology* **1978**;127:385–392
5. Drayer BP, Wolfson SK Jr, Reinmuth OM, Dujovny M, Boehnke M, Cooke EE. Xenon enhanced computed tomography for the analysis of cerebral integrity, perfusion, and blood flow. *Stroke* **1978**; 9:123–130
6. Harper AM, Bell RA. The effect of metabolic acidosis and alkalosis on the blood flow through the cerebral cortex. *J Neurol Neurosurg Psychiatry* **1963**;26:341–344
7. Meyer JS, Hata T, Imai A. Clinical and experimental studies of diaschisis. In: Wood JH, ed. *Cerebral blood flow: physiologic and clinical aspects.* New York: McGraw-Hill, **1987**:481–502
8. Harper AM. Autoregulation of cerebral blood flow: influence of the arterial blood pressure on the blood flow through the cerebral cortex. *J Neurol Neurosurg Psychiatry* **1966**;29:398–403
9. Lassen NA. Cerebral blood flow and oxygen consumption in man. *Physiol Rev* **1959**;39:183–238
10. Rapela CE, Green HD. Autoregulation of canine cerebral blood flow. *Circ Res* **1964**;15[suppl 1]:205–212
11. Jones TH, Morawetz RB, Crowell RN, et al. Thresholds of focal cerebral ischemia in awake monkeys. *J Neurosurg* **1981**;54:773–781
12. Baron JC, Bousser MG, Rey A, Guillard I, Comar D, Castaigne P. Reversal of focal "misery perfusion syndrome" by extraintracranial bypass in hemodynamic cerebral ischemia: a case study with ^{15}O positron emission tomography. *Stroke* **1981**;12:454–459
13. Gur D, Yonas H, Jackson DL, et al. Simultaneous measurements of cerebral blood flow by the xenon/CT method and the microsphere method: a comparison. *Invest Radiol* **1985**;20:672–677
14. Faturos PP, Wist AO, Kishore PRS. Xenon/computed tomography cerebral blood flow measurements: methods and accuracy. *Invest Radiol* **1987**;22:705–712
15. DeWitt DS, Faturos PP, Wist AO, et al. Stable xenon versus radiolabeled microsphere cerebral blood flow measurements in baboons. *Stroke* **1989**;20:1716–1723
16. Wolfson SK Jr, Clark J, Greenberg JH, et al. Xenon-enhanced computed tomography compared with [^{14}C]iodoantipyrine for normal and low cerebral blood flow states in baboons. *Stroke* **1990**;21:751–757
17. Yonas H, Gur D, Claasen D, Wolfson SK Jr, Moossy J. Stable xenon enhanced computed tomography in the study of clinical and pathologic correlates of focal ischemia in baboons. *Stroke* **1988**;19:228–238
18. Yonas H, Gur D, Claassen D, Wolfson SK Jr, Moossy J. Stable xenon-enhanced CT measurement of cerebral blood flow in reversible focal ischemia in baboons. *J Neurosurg* **1990**;73:266–273
19. Frackowiak RSJ, Lenzi G, Jones T, Heather JD. Quantitative measurement of regional cerebral blood flow and oxygen metabolism in man using [^{15}O] and positron emission tomography; theory, procedure, and normal values. *J Comput Assist Tomogr* **1980**;4:727–736
20. Rodriquez G, Warkentin S, Risberg J, Rosadini G. Sex differences in regional cerebral blood flow. *J Cereb Blood Flow Metab* **1988**;8:783–789
21. Melamed E, Lavy S, Bentin S, Cooper G, Rinot Y. Reduction in regional cerebral blood flow during normal aging in man. *Stroke* **1980**;11:31–35
22. Drayer BP, Gur D, Yonas H, Wolfson SK Jr, Cook EE. Abnormality of the xenon brain:blood partition coefficient and blood flow in cerebral infarction: an in vivo assessment using transmission computer tomography. *Radiology* **1980**:135:349–354
23. Hughes RL, Yonas H, Gur D, Latchaw RE. Cerebral blood flow determination within the first 8 hours of cerebral infarction using stable xenon-enhanced computed tomography. *Stroke* **1989**;20:754–760

24. Powers WJ, Grubb RL, Baker RP, Mintun MA, Raichle ME. Regional cerebral blood flow and metabolism in reversible ischemia due to vasospasm: determination by positron emission tomography. *J Neurosurg* **1985**;62:539–546
25. Darby JM, Yonas H, Gur D, Latchaw RE. Xenon-enhanced computed tomography in brain death. *Arch Neurol* **1987**;44:551–554
26. Darby JM, Yonas H, Brenner RP. Brainstem death with persistent EEG activity: evaluation by xenon-enhanced computed tomography. *Crit Care Med* **1987**;15:519–521
27. Ashwal S, Schneider S, Thompson J. Xenon computed tomography measuring cerebral blood flow in the determination of brain death in children. *Ann Neurol* **1989**;25:539–546
28. Koudstaal PJ, Stibbe J, Vermeulen M. Fatal ischaemic brain oedema after early thrombolysis with tissue plasminogen activator in acute stroke. *BMJ* **1988**;297:1571–1574
29. Becker RC, Gore JM. Tissue plasminogen activator and intracranial hemorrhage. *Ann Intern Med* **1990**;112:630
30. Suzuki R, Ohno K, Matsushima Y, Inaba Y. Serial changes in focal hyperemia associated with hypertensive putaminal hemorrhage. *Stroke* **1988**;19:322–325
31. Erba SM, Horton JA, Latchaw RE, et al. Balloon test occlusion of the internal carotid artery with stable xenon/CT cerebral blood flow imaging. *AJNR* **1988**;9:533–538
32. De Vries EJ, Sekhar LN, Horton JA, et al. A new method to predict safe resection of the internal carotid artery. *Laryngoscope* **1990**;100:85–88
33. Vorstrup S, Hendriksen L, Paulsen OB. Effect of acetazolamide on cerebral metabolic rate for oxygen. *J Clin Invest* **1984**;74:1634–1639
34. Rogg J, Rutigliano M, Yonas H, Johnson DW, Pentheny S, Latchaw RE. The acetazolamide challenge: imaging techniques designed to evaluate cerebral blood flow reserve. *AJNR* **1989**;10:803–810
35. Rutigliano MJ, Yonas H, Johnson DW. Natural history of patients with compromised cerebral reserves. *J Cereb Blood Flow Metab* **1989**;9:S609
36. Batjer HH, Devous MD, Purdy PD, Mickey B, Bonte FJ, Samson D. Improvement in regional cerebral blood flow and cerebral vasoreactivity after extracranial-intracranial arterial bypass. *Neurosurgery* **1988**;22:913–919
37. Symon L. Disordered cerebro-vascular physiology in aneurysmal subarachnoid hemorrhage. *Acta Neurochir* (Wein) **1978**;41:7–22
38. Fukai MB, Johnson DW, Yonas H, Sekhar L, Latchaw RE, Pentheny S. Time course, pattern, and severity of delayed cerebral ischemia after subarachnoid hemorrhage. *Neuroradiology* (in press)
39. Yonas H, Sekhar L, Johnson DW, Gur D. Determination of irreversible ischemia by xenon-enhanced computed tomographic monitoring of cerebral blood flow in patients with symptomatic vasospasm. *Neurosurgery* **1989**;24:368–372
40. Yonas H. Cerebral blood measurements in vasospasm. *Neurosurg Clin North Am* **1990**;1:307–317
41. Homan RW, Devous MD, Sokely EM, Bonte FJ. Quantification of intracerebral steal in patients with arteriovenous malformation. *Arch Neurol* **1986**;43:779–785
42. Okabe T, Meyer JS, Okayasu H. Xenon-enhanced CT CBF measurements in cerebral AVMs before and after excision. *J Neurosurg* **1983**;59:21–31
43. Marks MP, O'Donahue J, Fabricant JI, et al. Cerebral blood flow evaluation of arteriovenous malformations with stable xenon CT. *AJNR* **1988**;9:1169–1175
44. Marks MP, Lane B, Steinberg GK, Enzmann DR. Correlation of xenon CT and vascular architecture in patients with intracerebral AVMs and clinical symptoms of steal. *Proceedings of the 1st International Conference on Stable Xenon CT/CBF* (in press)
45. Tarr RW, Johnson DW, Rutigliano M, et al. Use of acetazolamide-challenge xenon CT in the assessment of cerebral blood flow dynamics in patients with arteriovenous malformations. *AJNR* **1990**;11:441–448
46. Batjer HH, Devous MD, Meyer YJ, Purdy PD, Samson DS. Cerebrovascular hemodynamics in arteriovenous malformation complicated by normal perfusion pressure breakthrough. *Neurosurgery* **1988**;22:503–509
47. Graham DI, Adams JH, Doyle D. Ischemic brain damage in fatal non-missile head injuries. *J Neurol Sci* **1978**;39:213–234
48. Yoshino E, Yamaki T, Higuchi T, et al. Acute brain edema in fatal head injury: analysis by dynamic CT scanning. *J Neurosurg* **1985**;63:830–839
49. Overgaard J, Mosdal C, Tweed WA. Cerebral circulation after head injury. Part 3: Does reduced regional cerebral blood flow determine recovery of brain function after blunt head injury? *J Neurosurg* **1981**;55:63–74
50. Mendelow AD, Teasdale GM, Russel T, et al. Effect of mannitol in cerebral blood flow and cerebral perfusion pressure in human head injury. *J Neurosurg* **1985**;63:43–48
51. Barclay L, Zemcov A, Reichert W, et al. Cerebral blood flow decrements in chronic head injury syndrome. *Biol Psychiatry* **1985**;20:146–157
52. Wozney P, Yonas H, Latchaw RE, Gur D, Good W. Central herniation revealed by focal decrease in blood flow without elevation of intracranial pressure: a case report. *Neurosurgery* **1985**;17:641–644
53. Obrist WD, Gennarelli TA, Segwa H, et al. Relation of cerebral blood flow to neurological status and outcome in head-injured patients. *J Neurosurg* **1979**;51:292–300
54. Obrist WD, Langfitt TW, Jaggi JL, Cruz J, Gennarelli TA. Cerebral blood flow and metabolism in comatose patients with acute head injury: relationship to intracranial hypertension. *J Neurosurg* **1984**;61:241–253
55. Muizelaar JP, Marmarou A, DeSalles AAF, et al. Cerebral blood flow and metabolism in severely head-injured children. Part 1: Relationship with GCS score, outcome, ICP, and PVI. *J Neurosurg* **1989**;71:63–71
56. Du Trevou MD, Bullock MRR, Van Dellen JR, Osborn IJS, Blake GTW, Barlow J. Regional cerebral blood flow determination by computed tomography and xenon gas inhalation after severe head injury: report of 2 cases. *S Afr J Surg* **1987**;25:95–98
57. Rosner MJ. Cerebral perfusion pressure: link between intracranial pressure and systemic circulation. In: Wood JH, ed. *Cerebral blood flow: Physiologic and clinical aspects*. New York: McGraw-Hill, **1987**:425–448
58. Saul TG, Ducker TB. Effect of intracranial pressure monitoring and aggressive treatment on mortality in severe head injury. *J Neurosurg* **1982**;56:498–503
59. Gorgon E, Rossanda M. Further studies in cerebrospinal fluid acid-base balance in patients with brain lesions. *Acta Anaesthesiol Scand* **1970**;14:79–109
60. Ward JD, Choi S, Marmarou R, et al. Effect of prophylactic hyperventilation on outcome in patients with severe head injury. In: Hoff JT, Betz AL, eds. *Intracranial pressure VII*. Berlin: Springer-Verlag, **1989**:630–633
61. Cold GE, Jensen FT, Malmros R. The effects of $Paco_2$ reduction on regional cerebral blood flow in the acute phase of brain injury. *Acta Anaesthesiol Scand* **1977**;21:359–367
62. Enevoldsen EM, Jensen FT. Autoregulation and CO_2 responses of cerebral blood flow in patients with acute severe head injury. *J Neurosurg* **1978**;48:689–703
63. Darby JM, Yonas H, Marion DW, Latchaw RE. Local "inverse steal" induced by hyperventilation in head injury. *Neurosurgery* **1988**;23:84–88
64. Yonas H, Snyder JV, Gur D, et al. Local cerebral blood flow alterations (Xe-CT method) in an accident victim. *J Comput Assist Tomogr* **1984**;8:990–991
65. Kety SS. The theory and applications of the exchange of inert gas at the lungs and tissues. *Pharmacol Rev* **1951**;3:1–41
66. Gur D, Herron JM, Molter BS, et al. Simultaneous mass spectrometry and thermoconductivity measurements of end-tidal xenon concentrations: a comparison. *Med Phys* **1984**;11:208–212
67. Latchaw RE, Yonas H, Pentheny SL, Gur D. Adverse reactions to xenon-enhanced CT cerebral blood flow determination. *Radiology* **1987**;163:215–254
68. Winkler S, Turski P, Holden J, Koeppe R, Rusy B, Garber E. Xenon effects on CNS control of respiratory rate and tidal volume—the danger of apnea. In: Hartmann A, Hoyer S, eds. *Cerebral blood flow and metabolism measurement*. Berlin: Springer-Verlag, **1985**:356–360
69. Obrist WD, Jaggi JL, Harel D, et al. Effect of stable xenon inhalation on human CBF. *J Cereb Blood Flow Metab* **1985**;5:557–558
70. Kearfott KJ, Lu HC, Rottenberg DA, et al. The effects of CT drift on xenon/CT measurement of regional cerebral blood flow. *Med Phys* **1984**;11:686–689